HHS Public Access

Author manuscript

Circulation. Author manuscript; available in PMC 2022 January 12.

Published in final edited form as:

Circulation. 2021 January 12; 143(2): 145–159. doi:10.1161/CIRCULATIONAHA.120.049813.

A novel endocrine role for the BAT-released lipokine 12,13-diHOME to mediate cardiac function

Kelsey M. Pinckard, M.S.[1,2,#], **Vikram K. Shettigar, Ph.D.**[1,2,#], **Katherine R. Wright, M.P.H.**[1,2], **Eaman Abay, B.S.**[1,2], **Lisa A. Baer, M.S.**[1,2], **Pablo Vidal, M.S.**[1,2], **Revati S. Dewal, M.S.**[1,2], **Devleena Das, B.S.**[3], **Silvia Duarte-Sanmiguel, Ph.D.**[3,4], **Diego Hernández-Saavedra, Ph.D.**[1,2], **Peter J. Arts, M.S.E.**[1,2], **Adam C. Lehnig, B.S.**[1,2], **Valerie Bussberg, B.S.**[5], **Niven R. Narain, Ph.D.**[5], **Michael A. Kiebish, Ph.D.**[5], **Fanchao Yi, Ph.D.**[6], **Lauren M. Sparks, Ph.D.**[6], **Bret H. Goodpaster, Ph.D.**[6], **Steven R. Smith, M.D.**[6], **Richard E. Pratley, M.D.**[6], **E. Douglas Lewandowski, Ph.D.**[1,6,7,8], **Subha V. Raman, M.D.**[1,8], **Loren E. Wold, Ph.D.**[1,2,9], **Daniel Gallego Perez, Ph.D.**[1,3,10], **Paul M. Coen, Ph.D.**[6], **Mark T. Ziolo, Ph.D.**[1,2,8,#,*], **Kristin I. Stanford, Ph.D.**[1,2,8,#,*,$]

[1]Dorothy M. Davis Heart and Lung Research Institute, The Ohio State University Wexner Medical Center, Columbus, OH 43210

[2]Department of Physiology and Cell Biology, The Ohio State University College of Medicine, Columbus, OH 43210

[3]Department of Biomedical Engineering, The Ohio State University, Columbus, OH 43210

[4]Department of Nutrition, The Ohio State University, Columbus, OH 43210

[5]BERG, Framingham, Massachusetts 01701, USA

[6]Translational Research Institute for Metabolism and Diabetes, AdventHealth, Orlando, Florida 32804

[7]Sanford Burnham Prebys Medical Discovery Institute at Lake Nona, Orlando, Florida 32827

[8]Department of Internal Medicine, The Ohio State University College of Medicine, Columbus, OH 43210

[9]College of Nursing, The Ohio State University, Columbus, OH 43210

[10]Department of Surgery, The Ohio State University College of Medicine, Columbus, OH 43210

Abstract

Background: Brown adipose tissue (BAT) is an important tissue for thermogenesis, making it a potential target to decrease the risks of obesity, type 2 diabetes, and cardiovascular disease (CVD), and recent studies have also identified BAT as an endocrine organ. While BAT has been implicated

[*]To whom correspondence should be addressed: Kristin I. Stanford, 460 W. 12th Ave., Columbus, OH 43210, Phone: 614-247-8287, kristin.stanford@osumc.edu; Mark T. Ziolo, 333 W. 10th Ave., Columbus, OH 43210, Phone: 614-688-7905, mark.ziolo@osumc.edu.
[#]Contributed equally
[$]Lead Contact

Disclosures
None.

to be protective in cardiovascular disease, to this point there are no studies that identify a direct role for BAT to mediate cardiac function.

Methods: To determine the role of BAT on cardiac function, we utilized a model of BAT transplantation. We then performed lipidomics and identified an increase in the lipokine, 12,13-diHOME. We utilized a mouse model with sustained overexpression of 12,13-diHOME and investigated the role of 12,13-diHOME in a $NOS1^{-/-}$ mouse and in isolated cardiomyocytes to determine effects on function and respiration. We also investigated 12,13-diHOME in a cohort of human patients with heart disease.

Results: Here, we determined that transplantation of BAT (+BAT) improves cardiac function via the release of the lipokine 12,13-diHOME. Sustained overexpression of 12,13-diHOME using tissue nanotransfection negated the deleterious effects of a high-fat diet on cardiac function and remodeling, and acute injection of 12,13-diHOME increased cardiac hemodynamics via direct effects on the cardiomyocyte. Furthermore, incubation of cardiomyocytes with 12,13-diHOME increased mitochondrial respiration. The effects of 12,13-diHOME were absent in *NOS1*$^{-/-}$ mice and cardiomyocytes. We also provide the first evidence that 12,13-diHOME is decreased in human patients with heart disease.

Conclusion: Our results identify an endocrine role for BAT to enhance cardiac function that is mediated by regulation of calcium cycling via 12,13-diHOME and NOS1.

Keywords

brown adipose tissue (BAT); exercise; lipokines; 12,13-diHOME; cardiac function; NOS1

Introduction

Cardiovascular disease (CVD) is the leading cause of death across the U.S. and worldwide[1] and affects almost half of all adults in the United States. CVD encompasses a wide range of conditions that affect the heart and vasculature including arrhythmias, dilated, hypertrophic, or idiopathic cardiomyopathies, heart failure and atherosclerosis[1], which can lead to fatal cardiac events such as stroke, myocardial infarction, or cardiac arrest. CVD can arise in response to multiple factors, including obesity. Obesity is an independent risk factor for the development of CVD and elevates the risk of CVD by increasing the development and severity of comorbidities such as hypertension, dyslipidemia, and diabetes[2].

An important therapeutic tool to combat CVD, obesity, and type 2 diabetes is exercise[3-8]. Exercise remodels the heart into an “athlete’s” heart, which includes physiological hypertrophy and enhanced systolic and diastolic function[9]. This remodeling is protective to the heart, prevents the onset and development of CVD, and reflects direct modifications of the cardiomyocyte. Our previous work has indicated that nitric oxide (NO) via NO synthase type 1 (NOS1) is essential for the exercise-induced effects on the cardiomyocyte[10].

Brown adipose tissue (BAT) is an important therapeutic tool to combat obesity and type 2 diabetes. In response to BAT transplantation[11, 12], cold exposure[13], or exercise[14-16], BAT acts in an endocrine manner to affect whole-body metabolism and function. BAT releases ‘batokines’ including proteins[11, 17, 18] and lipokines[13, 14] which improve glucose and fatty

acid metabolism. In response to exercise and cold exposure, BAT releases the lipokine 12,13-diHOME, an oxidized linoleic acid metabolite. 12,13-diHOME acts in an autocrine and endocrine manner to increase fatty acid uptake into both BAT and skeletal muscle, reduces circulating triglycerides, and is negatively correlated with adiposity and insulin resistance in humans[13, 14]. Studies have indicated that BAT activity is increased in CVD[19-21] and that this may have a protective effect, however no studies have investigated if BAT directly mediates cardiac function.

Here, we identified a direct role for BAT on cardiac function mediated via 12,13-diHOME. Sustained upregulation of 12,13-diHOME by tissue nanotransfection (TNT) negated the adverse effects of a high-fat diet on cardiac function and remodeling, identifying this molecule as a potential therapeutic. Acute treatment with 12,13-diHOME increased cardiac hemodynamics via direct effects on the cardiomyocyte. Furthermore, incubation of cardiomyocytes with 12,13-diHOME increased mitochondrial respiration, and these effects were absent in *NOS1*$^{-/-}$ mice and cardiomyocytes, providing a new mechanism of action for 12,13-diHOME and NOS1. We further identified a role for 12,13-diHOME in human patients by determining that 12,13-diHOME is decreased in patients with heart disease and that this was correlated with lower ejection fraction. Our results suggest a direct endocrine role for BAT to enhance cardiac function and, for the first time, indicate that this is mediated by regulation of calcium cycling via 12,13-diHOME and NOS1.

Experimental Methods

Data Availability

The data, analytic methods, and study materials that support the findings of this study are available from the corresponding author upon reasonable request. Correspondence and requests for materials should be addressed to K.I.S.

Human study protocols

The human study protocols for blood collection, assays and cardiac function data from clinical patients were approved by the AdventHealth Institutional Review Board (IRBNet# 936207, 238153, and 500423) and The Ohio State University Medical Center Institutional Review Board. Study participants were recruited from The Florida Hospital Cardiovascular Institute and Transplant Institute Participants and were recruited by the study coordinator through electronic medical record (EMR) searches to identify those undergoing LVAD implantation and explanation, heart transplant, valve replacement or repair, endomyocardial biopsy during catheterization of patients with idiopathic heart failure, and arterial bypass procedures (CABG). Prior to the procedure, potential participants > 18 years of age were informed about the study and if they expressed an interest, the study coordinator consented them. All patients provided written informed consent before inclusion in the study. Fasting blood samples were drawn from an antecubital vein from patients with clinical indices of heart failure (males: n=17; BMI=26.5±2.7; age=65.4±2.4; females: n=7; BMI=26.1±1.9; age=62.4±7.1) and from volunteers without heart failure (males: n=25; BMI=24.8±1.1; age=56.3±4.4; females: n=26; BMI=23.4±0.4; age=43.2±3.1). Blood was drawn into a potassium EDTA blood tube and processed per the manufacturer’s instructions. Plasma

aliquots were stored at −80°C for lipidomics analysis. Ejection fraction (EF) was measured using standard cardiac magnetic resonance cine imaging, computing EF from contiguous short-axis cine images by semi-automated delineation of endocardial contours at end-systole and end-diastole (cvi42, Circle Cardiovascular Imaging, Calgary).

Mice and treatments

All animal procedures were approved by the Institutional Animal Use and Care Committee at The Ohio State University. Transplantation of brown adipose tissue (BAT) was performed as previously described[11] using BAT removed from the intrascapular region of 12-week-old male C57BL/6 mice (Charles River Laboratories). After euthanasia of donor mice by cervical dislocation, BAT was removed and incubated in 10 ml saline at 37°C for 20–30 minutes. Twelve-week-old C57BL/6 recipient mice were anesthetized by isoflurane inhalation in oxygen (3% isoflurane in 97% oxygen). For each recipient mouse, 0.1g donor BAT was transplanted into the visceral cavity. The transplant was carefully lodged deep between folds within the endogenous epididymal fat of the recipient [22]. Mice that were sham operated underwent the same procedure, but instead of receiving BAT, their epididymal fat pad was located, exposed, and then replaced.

Exercise Training Paradigm

To achieve exercise-induced adaptations on cardiac function, wild-type mice underwent an interval-based treadmill training protocol for 8 wks (Table I in the Supplement)[10].

Oral gavage of sEH inhibitors

C57BL/6 male mice (Charles River Laboratories) were fed a normal chow diet before and throughout the experiment. Sham and +BAT mice underwent daily oral gavage of sEH inhibitors beginning 10 weeks after the transplant or sham surgery. Mice underwent daily oral gavage with vehicle (Phosphate Buffer Saline [PBS]), or 25mg/L AUDA in PBS (Cayman Chemicals #10007927), or 50mg/L t-AUCB in PBS (Cayman Chemicals #16568). Mice were gavaged at 0.5mg/kg daily for 14–16 days.

TNT device fabrication

Tissue Nano-Transfection (TNT) devices were fabricated from double side polished Silicon (Si) wafers, as reported previously[23]. Briefly, projection lithography was used to define 400–500 nm on a photoresist. Deep reactive ion etching (DRIE) was then used drill nanochannels through the exposed Si surface. The backside of the wafers was then patterned with an array of 50 μm openings via standard photolithography followed by DRIE to gain fluidic access to the nanochannels. Finally, a 50 nm thick insulating layer of Si_3N_4 was deposited on the wafers via PECVD.

TNT-based plasmid delivery

Six week old male, C57BL/6 mice were placed on a high-fat diet (60% kcal/fat) (Research Diets, Inc.) for 6 weeks prior to TNT treatment. They remained on high-fat diet throughout the TNT treatment. All plasmids (UCP1, Ephx1, Ephx2) were purchased from Origene and expanded in Escherichia coli following standard procedures. Prior to TNT, each plasmid was

diluted in PBS to a final concentration of 0.05 μg/μl, and loaded into the plasmid reservoir of the TNT device. The fur was removed and the skin was exfoliated as described previously[23]. The TNT device was then put in contact with the skin, juxtaposed to an intradermal positive electrode. The negative electrode was inserted into the plasmid reservoir, and a pulsed electric field (250 V, 10 ms pulses, 10 pulses) was applied across electrodes. Approximately 2–3 cm^2 were TNT-treated per mouse. This procedure was conducted directly on the skin that overlays suprascapular and inguinal BAT and WAT deposits, respectively[24], and was repeated weekly for a total of 8 weeks.

Lipidomic profiling and 12,13-diHOME quantification

All lipid standards were purchased from the Cayman Chemical Company. C_{18}SPE cartridges were purchased from Biotage. All solvents are of high-performance liquid chromatography (HPLC) or LC/MS grade and were acquired from Sigma-Aldrich, Fisher Scientific or VWR International. Aliquots of 100 μl serum were used for analysis. The samples were prepared as previously described[13]. MS analysis was performed on a SCIEX TripleTOF 6600+ system using the HR-MRM strategy consisting of a time of flight (TOF) MS experiment looped with multiple MS/MS experiments as previously described[13]. The identity of a component was confirmed using PeakView software (SCIEX), and quantification was performed using MultiQuant software (SCIEX). The quantification of 12,13-diHOME was performed against a standard calibration curve built with fifteen points ranging from 0.01 pg/μl to 1000 pg/μl. Obtained values were corrected with the corresponding internal standard. All measurements were performed in a blinded fashion.

Measurements of Cardiomyocyte Sarcomere Function and Calcium Transient

Cardiomyocytes were isolated from wild-type C57BL/6 male mice (Charles River) or *NOS1*$^{-/-}$ mice (B6;129S4-*Nos1*^{tm1Plh}/J; stock no. 002633; Jackson Labs). Unloaded cardiomyocyte function (sarcomere shortening, kinetics and Ca2+ transients) were measured as previously performed[25, 26]. In brief, hearts were rapidly excised and cannulated on a constant-flow Langendorff perfusion apparatus, and perfused via the aorta at 37° C with buffer containing (in mM) 113 NaCl, 4.7 KCl, 0.6 KH2PO4, 0.6 Na2HPO4, 1.2 MgSO4, 12.4 BMD, 12 NaHCO3, 10 KHCO3, 10 HEPES 1M, and 30 Taurine, followed by digestion with liberase enzyme (0.25 mg/ml)[27, 28]. After perfusion and digestion ventricles were removed and minced (under sterile conditions), filtered, and equilibrated with 1 mM $CaCl_2$ and FBS at room temperature[27, 28]. Cardiomyocytes were plated on laminin-coated glass slides and placed on the stage of an inverted Olympus IX-71 microscope and superfused (~1 ml/min at 30° C) with contractile buffer containing (in mM, pH 7.4) 4 KCl, 131 NaCl, 1 MgCl2, 10 HEPES, 1 CaCl2, and 10 glucose[29]. The cells were visualized using a 40× objective and field-stimulated at 1 Hz for 3 ms using a Myopacer Field-Stimulator system[29, 30]. Sarcomere length, time to contraction/relaxation and contraction/relaxation kinetics will were recorded using the IonOptix video imaging system and a Myocam-S Digital charge-coupled device camera. Changes in intracellular Ca^{2+} levels were monitored using (0.5 μM) Fura-2 dual-excitation (360/380 nm) single emission (510 nm) ratiometric imaging[29, 30]. Measurements were taken at baseline and with acute superfusion of 10μM 12,13-diHOME.

Seahorse bioanalyzer

Cardiomyocytes were isolated from 12–24 week old male C57BL/6 male (Charles river) or *NOS1*$^{-/-}$ mice (B6;129S4-*Nos1*^{tm1Plh}/J; stock no. 002633; Jackson Labs), chow fed mice. Isolated cardiomyocytes (25,000 per well) were seeded onto laminin-coated Seahorse Plates (Agilent) according to standard protocols. Cells were treated for 1 h with 10 μM 12,13-diHOME or were untreated. The oxygen-consumption rates (OCR; indicating mitochondrial respiration) and extracellular acidification rates (ECAR; indicating glycolysis rate) were monitored in a Seahorse XF24 instrument using the standard protocol of 3-min mix, 2-min wait and 3-min measure [31]. Carbonyl cyanide-p-trifluoromethoxy-phenyl-hydrazon (FCCP; 2 μM) was used to determine the cells maximal respiratory capacity by allowing the electron transport chain to function at its maximal rate (maximal respiratory capacity is derived by subtracting non-mitochondrial respiration from the FCCP rate). Oligomycin (a complex V inhibitor; 2 μM) was used to derive ATP-linked respiration (by subtracting the oligomycin rate from baseline cellular OCR) and proton leak respiration (by subtracting non-mitochondrial respiration from the oligomycin rate). AntimycinA/Roteone (mitochondrial inhibitors; 0.5 μM) was used to determine non-mitochondrial respiration. For mechanistic experiments, cells were treated for 1 h with tetracaine (specific RyR inhibitor; 1mM), 2,3-butanedione monoxime (BDM; myosin-ATPase inhibitor; 10 μM) and nifedipine (L-type calcium channel inhibitor; 10 μM) were used. Data from wells of the same treatment group were averaged together and analyzed directly using Waves software. For the normalization of respiration to protein content, cells were lysed in RIPA buffer and protein concentration was measured by Bradford assay.

Cardiomyocyte Fatty Acid Uptake

Cardiomyocytes were isolated from 12–24 week old male *LucTg* (FVB-Tg(CAG-luc,-GFP)L2G85Chco/J; stock no. 008450; Jackson Labs) chow-fed mice. Isolated cardiomyocytes (50,000 cells per well) were seeded onto laminin-coated 12-well plates according to standard protocols in FBS-free media for one hour. After one hour of serum-starve, 10μm FFA-SS-Luc (Intrace Medical) conjugated probe was added to each well with or without 10μM 12,13-diHOME directly before imaging using the IVIS Spectrum for fluorescent optical imaging using sequential 3 min exposures for 30 min. Data was analyzed using Living Image Software, and movies were assembled from individual images using ImageJ.

In vivo cardiac function

Wild-type C57BL/6 male mice (Charles river) or *NOS1*$^{-/-}$ mice (B6;129S4-*Nos1*^{tm1Plh}/J; stock no. 002633; Jackson Labs) were anesthetized with 1–2% isoflurane and echocardiography was conducted using a Vevo 2100 Ultrasound. Echocardiogram data was analyzed using VevoLab software to determine left ventricle (LV) ejection fraction, LV mass, and LV diastolic diameter.

Cardiac pressure-volume analysis

Hemodynamic, systolic, and diastolic measurements performed as previously done[32, 33]. Briefly, mice were anesthetized with 1% isoflurane and a 1.4 F Millar catheter was advanced

from the carotid artery into the left ventricle. LV pressure-volume dynamics were simultaneously measured over a wide range of heart rates (240–600bpm)[32]. For the TNT experiments, since there were different baseline heart rates, data was normalized to the lowest heart rate. For the acute injection experiments, 12,13-diHOME, 9,10-diHOME, or 9-HODE were infused through the femoral vein (all at 1.5 μg/kg). All pressure-volume loop parameters were calculated using PV loop analysis software module for Lab Chart on ADInstruments.

Statistical Analysis

The data are presented as means ± SEM. Statistical significance was defined as $P < 0.05$ and determined by one- or two-way ANOVA, or repeated measures two-way ANOVA, with Tukey and Bonferroni post hoc analysis, or unpaired two-tailed Student's t-test. For experiments with human subjects, linear regression analyses were used for analysis. Kolmogorov-Smirnov test were used for normality tests.

Results

Transplantation of BAT and Exercise improve cardiac function in mice

To determine the effects of increasing BAT mass by transplantation on cardiac function, mice were transplanted with 0.1g BAT (+BAT) into the visceral cavity from age and gender matched control mice. Twelve weeks post-transplantation, *in vivo* cardiac hemodynamics revealed that +BAT mice had improved systolic function (Fig. 1A). We measured dP/dt_{min} and determined a more negative dP/dt_{min} in +BAT mice, indicating accelerated relaxation, and thus enhanced diastolic function (Fig. 1B) compared to Sham mice. +BAT did not alter ejection fraction (1C), but resulted in beneficial cardiac remodeling (Fig. 1D-F; Table II in the Supplement).

It is well-established that exercise-training influences cardiac function[7, 8, 34-36], and our laboratory has recently identified a role for exercise to influence the endocrine function of BAT[14]. To determine if exercise and +BAT resulted in similar adaptations to cardiac function, a group of Sham-operated surgical control mice underwent 8 weeks of intense exercise interval training beginning four weeks post-surgery, and cardiac function was assessed. Both exercise and +BAT had similar improvements on *in vivo* cardiac hemodynamics (Fig. 1A-B) but no change in ejection among groups (Fig. 1C), similar to what has been previously reported[37]. Markers of cardiac remodeling, including end diastolic volume (EDV), left ventricular mass (LVM), and diastolic diameter were increased with both exercise and +BAT (Fig. 1D-F). To determine changes in contractility were also involved, we normalized for EDV. When normalized, an increase in contractility contributed to the enhanced systolic function (Figure I A in the Supplement). Taken together these data indicate that both exercise and +BAT have a similar effect to improve cardiac function via preload (EDV) and contractility in mice.

Exercise and +BAT improve metabolic health

Given our previous data indicating that +BAT improves metabolic health in mice[11, 14], we examined the effects of +BAT and exercise on glucose tolerance and body composition.

Metabolic testing was performed at the same time as *in vivo* cardiac function testing and revealed that both exercise and +BAT improved glucose tolerance (Figure I B-C in the Supplement). Exercise-training decreased body weight (Figure I D in the Supplement), and both exercise and +BAT decreased % fat mass and increased % lean mass (Figure I E-F). There was a minimal effect of +BAT or exercise on Vo_2, Vco_2, respiratory exchange ratio (RER), heat and energy expenditure, or spontaneous activity (Figure I G-K in the Supplement). These data indicate that both exercise and +BAT improve glucose tolerance and decrease % fat mass to a similar extent.

12,13-diHOME is up-regulated with +BAT and Exercise.

Given the putative endocrine role of BAT[18] and our recent studies identifying the effect of exercise to alter the signaling lipidome[13, 14], we examined the effect of exercise and +BAT on circulating signaling lipokines. Plasma was analyzed by liquid chromatography tandem mass spectrometry (LC-MS/MS) to measure the concentrations of a panel of 90 mediator lipids with annotated signaling properties (Complete lipidomics data will be submitted to https://www.metabolomicsworkbench.org/ upon publication). Hierarchical clustering revealed similarities between +BAT and Sham-Exercised, but no clear pattern of lipokine regulation among Sham-Sedentary, +BAT, or Sham-Exercised mice (Fig. 2A; Figure I L in the Supplement). Eleven signaling lipids were increased in +BAT mice (Fig. 2B, Table III in the Supplement) and 4 signaling lipids were increased with exercise (Fig. 2C, Table IV in the Supplement). Of these, there were three of the same lipokines increased among +BAT and exercise: 12,13-diHOME, 9,10-diHOME, and 9-HODE (Fig. 2D-F). Interestingly, the signaling lipid that was the most significantly increased by p-value and fold change in both the +BAT and exercised mice was 12,13-diHOME (Fig. 2B-D).

12,13-diHOME increases in vivo cardiac hemodynamics

Both +BAT and exercise improved cardiac function in mice and increased circulating 12,13-diHOME. To determine if 12,13-diHOME was responsible for the improved cardiac function in +BAT and exercise-trained mice, mice were acutely injected with 12,13-diHOME and *in vivo* cardiac hemodynamics were measured. Acute treatment of 12,13-diHOME improved systolic function (Fig. 3A; Figure II A in the Supplement) and diastolic function (Fig. 3B; Figure II B in the Supplement) compared to mice injected with saline. There was no effect of 9,10-diHOME or 9-HODE to alter systolic (Fig. 3A; Figure II A in the Supplement) or diastolic function (Fig. 3B; Figure II B in the Supplement). These data suggest that 12,13-diHOME is a potent positive inotropic and lusitropic modulator in mice.

sEH inhibition negates the improvement in cardiac function with BAT.

After observing the effect of 12,13-diHOME to acutely increase *in vivo* cardiac hemodynamics, we investigated if inhibition of 12,13-diHOME prevented the BAT-induced improvements in cardiac function. To do this, mice were divided into either Sham or +BAT, and 10 weeks after surgery fed daily via oral gavage with the soluble epoxide hydrolase (sEH) inhibitors AUDA or t-AUCB for 2 weeks. sEH are the enzymes that produce 12,13-diHOME. In the presence of sEH inhibitors, there was no effect of +BAT to improve cardiac function (Fig. 3C-F). These data provide further evidence that the improvements in cardiac function via BAT are mediated through sEH, and likely 12,13-diHOME.

Sustained treatment with 12,13-diHOME negates the deleterious effects of a high-fat diet on cardiac structure and function.

To test the therapeutic applications of 12,13-diHOME, mice were placed on a high-fat diet for 6 wks and tissue nanotransfection (TNT)[23] was performed using plasmids that expressed proteins of interest. These plasmids were electroplated on the skin that overlays BAT and WAT depots once a week for 8 wks to drive sustained expression of soluble epoxide hydrolase 1 and 2 (Ephx1/2; TNT-Ephx1/2) or uncoupling protein 1 (Ucp1; TNT-Ucp1). Ephx1/2 was selected because it is an important enzyme for the biosynthesis of 12,13-diHOME. 12,13-diHOME is regulated by soluble epoxide hydrolases (sEH) of which Ephx1 and Ephx2 are the major isoforms expressed in adipose tissue[13]. After the conversion of linoleic acid by cytochrome P450 to 12,13-epOME, Ephx1/2 are soluble epoxide hydrolases (sEH) that catalyze the conversion of 12,13-epOME to 12,13-diHOME. As such, TNT-driven overexpression of Ephx1 and 2 should correlate with increased synthesis of 12,13-diHOME in overlaying skin and circulation[38-40]. TNT-driven overexpression of UCP1 (TNT-Ucp1) was used as a proxy for BAT-mediated activity since UCP1 is the predominant marker of BAT and plays an important role in non-shivering thermogenesis. To confirm effectiveness of TNT-Ucp1, *Ucp1* was measured in skin, BAT, and perigonadal white adipose tissue (pgWAT). *Ucp1* was significantly increased in skin and BAT of TNT-Ucp1 mice (Figure II C in the Supplement). Control mice (TNT-Sham) underwent a sham procedure of weekly anesthetization only. Signaling lipids were measured (Figure II D in the Supplement) and TNT-Ephx1/2 increased 12,13-diHOME in circulation, but 12,13-diHOME was not altered in TNT-Ucp1 mice (Fig. 3G). All mice were compared to a baseline group; chow-fed, aged matched mice, in order to account for the effects both high-fat diet and TNT. Similar to previous studies, a high-fat diet resulted in adverse cardiac remodeling as observed by a decrease in ejection fraction (Fig. 3H) and an increase in posterior wall thickness and left ventricular mass in the TNT-Sham mice (Fig. 3I,J; Table V in the SupplementTNT-Ucp1 mice also had significant chamber dilation and end diastolic volume (Fig. 3K,L; Table V in the Supplement). However, TNT-Ephx1/2 mice were completely protected from the pathological remodeling induced by high-fat diet (Fig. 3I-L; Table V in the Supplement). Investigation of *in vivo* cardiac hemodynamics revealed that although systolic and diastolic function were not different (Figure II E-F in the Supplement), the TNT-Ephx1/2 mice maintained the force frequency response in systole (Fig. 3M) and diastole (Fig. 3N), indicating increased function with an increasing heart rate. The force frequency response was blunted in systole and diastole in the TNT-Sham and TNT-Ucp1 mice, consistent with what is observed in heart disease and type 2 diabetes (Fig. 3M,N)[41, 42]. To ascertain if these differences could be due to an increase in contractility, the data were normalized to EDV. Contractility was increased in TNT-Ephx1/2 mice compared to both Sham and TNT-UCP1 mice (Figure II G in the Supplement). These data indicate that an increase in TNT-Ephx1/2 negated the deleterious effects of a high-fat diet on cardiac function and remodeling. High-fat diet significantly increased body weight in the TNT-Sham and TNT-Ucp1 mice, but TNT-Ephx1/2 mice were protected from the high-fat diet-induced weight gain (Figure II H in the Supplement). TNT-Ephx1/2 mice also had decreased % fat mass, and increased % lean mass, compared to other groups (Figure II I,J in the Supplement). There was no effect of increasing TNT-Ephx1/2 or TNT-Ucp1 on glucose tolerance (Figure II K,L in the Supplement), similar to previous studies investigating the

effects of two weeks of chronic injection of 12,13-diHOME[13]. Together these data highlight the importance of the endocrine role for BAT to have a protective effect on cardiac structure and function, as TNT-driven modulation of Ucp1 expression resulted in adverse cardiac remodeling, while an increase in 12,13-diHOME (TNT-Ephx1/2) was protective.

12,13-diHOME increases contractile function and calcium uptake in isolated cardiomyocytes

After determining an increase in contractility observed *in vivo*, we further investigated if 12,13-diHOME had a direct effect on the function of isolated cardiomyocytes. Acute superfusion with 12,13-diHOME increased peak cardiomyocyte shortening (Fig. 4A) via an increase in Ca2+ transient amplitude (Fig. 4B). 12,13-diHOME also resulted in faster kinetics determined as greater maximal velocity of shortening (+dL/dt)(Fig. 4C), and maximal velocity of relengthening (-dL/dt)(Fig. 4D). These data indicate that 12,13-diHOME directly increases cardiomyocyte function via enhanced Ca^{2+} handling, consistent with the *in vivo* data indicating that 12,13-diHOME is a positive inotrope.

12,13-diHOME increases fatty acid uptake in cardiomyocytes.

Previous studies have indicated a role for 12,13-diHOME to increase fatty acid uptake[13, 14]. To test the hypothesis that 12,13-diHOME increases fatty acid uptake in cardiomyocytes, we isolated cardiomyocytes constitutively expressing luciferase *in vitro*. Cells were treated with FFA-SS Luc, a fatty acid conjugated to luciferin[43, 44], in the presence of 12,13-diHOME or a vehicle control. Fatty acid uptake was significantly elevated in isolated cardiomyocytes treated with 12,13-dihOME after 30 min of incubation (Fig. 4E; Supplemental Video 1). These data indicate that 12,13-diHOME increases fatty acid uptake in cardiomyocytes, similar to its effect on BAT and skeletal muscle[13, 14].

12,13-diHOME increases respiration in cardiomyocytes.

Based on previous data indicating that 12,13-diHOME increases mitochondrial function in BAT and skeletal muscle[13, 14], we hypothesized that 12,13-diHOME regulated mitochondrial function in cardiomyocytes. 12,13-diHOME increased basal oxygen consumption rates (OCR), maximal respiratory capacity, and non-mitochondrial respiration in isolated cardiomyocytes (Fig. 4F-I).

To determine if 12,13-diHOME increased mitochondrial respiration directly or indirectly via greater energy demand due to increased contraction, we measured OCR in cardiomyocytes incubated with 12,13-diHOME and the myosin inhibitor 2,3-Butanedione monoxime (BDM). Inhibition of myosin did not prevent 12,13-diHOME to increase basal OCR or maximal respiration, but prevented the increase in non-mitochondrial respiration (Fig. 4J-M). These data indicate that 12,13-diHOME increases respiration in cardiomyocytes.

Mechanism of action of 12,13-diHOME in cardiac function

We next investigated the mechanism through which 12,13-diHOME modulates cardiomyocyte function and respiration. Our previous work has shown that nitric oxide (NO) production via NO synthase type 1 (NOS1) is essential for the beneficial effects of exercise to the heart[10]. Since +BAT had similar effects on the heart as exercise, we hypothesized that

12,13-diHOME may function through a similar mechanism. Mice deficient in NOS1 (*NOS1*$^{-/-}$) were acutely injected with 12,13-diHOME and *in vivo* cardiac hemodynamics were measured. In contrast to what was observed in wild-type (WT) mice (Fig. 3A,B), there was no effect of acute injection of 12,13-diHOME on systolic (Fig. 5A; Figure III A in the Supplement) or diastolic (Fig. 5B; Figure III B in the Supplement) function in *NOS1*$^{-/-}$ mice. In addition, 12,13-diHOME had no effect on *NOS1*$^{-/-}$ cardiomyocyte peak shortening, Ca2+ transients, or kinetics (Fig. 5C-F). These data indicate that 12,13-diHOME confers beneficial effects on cardiac function via activation of NOS1.

In *NOS1*$^{-/-}$ cardiomyocytes there was no effect of 12,13-diHOME to increase basal oxygen consumption rates (OCR), maximal respiratory capacity, and non-mitochondrial respiration in cardiomyocyte (Fig. 5G-J). Since previous work indicated that NOS1 signaling activates the ryanodine receptor (RyR), we further investigated if RyR was involved in the 12,13-diHOME signaling pathway. Cardiomyocytes isolated from wild-type mice were incubated with 12,13-diHOME and the RyR2 inhibitor, tetracaine. 12,13-diHOME increased basal OCR in the presence or absence of tetracaine (Fig. 5K,L), but incubation with tetracaine blunted the effect of 12,13-diHOME on maximal respiration and non-mitochondrial respiration (Fig. 5K,M,N). Increasing Ca^{2+} cycling within the cardiomyocyte increases mitochondrial respiration[45], and inhibiting RyR via tetracaine prevents the increase in Ca^{2+} cycling and thus maximal respiration. This is consistent with the decrease in maximal respiration observed in cardiomyocytes treated with tetracaine, independent of 12,13-diHOME. Thus, our data indicate that 12,13-diHOME increases maximal mitochondrial respiration, via enhanced Ca^{2+} cycling. Together these data indicate that 12,13-diHOME increases cardiomyocyte contraction and respiration via a NOS1-dependent mechanism, and cardiomyocyte contraction is likely mediated via RyR (Figure 5O).

12,13-diHOME is decreased in human heart disease patients.

To determine if there was a correlation between 12,13-diHOME and heart disease or cardiac function in humans we measured 12,13-diHOME in a cohort of 75 male and female subjects, with or without heart disease. This cohort consisted of healthy males (n=25; BMI=24.8±1.1; age=56.3±4.4), healthy females (n=26; BMI=23.4±0.4; age=43.2±3.1), males with heart disease (n=17; BMI=26.5±2.7; age=65.4±2.4), and females with heart disease (n=7; BMI=26.1±1.9; age=62.4±7.1) (Table IV in the Supplement). Interestingly, both male and female subjects with heart disease had reduced concentrations of 12,13-diHOME (Fig. 6A). There was no difference in BMI among groups (Fig. 6B), but 12,13-diHOME was negatively correlated to BMI consistent with previous studies (Fig. 6C)[13, 14]. There was no difference in age among groups (Fig. 6D) and age was not correlated to 12,13-diHOME in this cohort of human subjects (Fig. 6E). Functional cardiac measurements were obtained in a subset of patients with heart disease, and these data revealed that ejection fraction (Fig. 6F) and fractional shortening (Fig. 6G) were positively correlated with 12,13-diHOME, indicating an important role for 12,13-diHOME to have a protective effect on cardiac function.

Discussion

Here, we establish a novel paradigm in which BAT plays a critical endocrine role to directly affect cardiac function and metabolism via 12,13-diHOME. 12,13-diHOME improves *in vivo* cardiac hemodynamics by increasing cardiomyocyte contraction, relaxation, and mitochondrial respiration. Sustained treatment with 12,13-diHOME negates the deleterious effects of a high-fat diet on cardiac function and remodeling, an effect that was not seen in TNT-Ucp1 mice. We further identified that 12,13-diHOME mediates these beneficial effects through the activation of NOS1. Human patients with heart disease had decreased concentrations of 12,13-diHOME, and 12,13-diHOME was directly correlated to ejection fraction in these patients. These data demonstrate an important mechanism for the endocrine role of BAT to mediate cardiac function in health and disease through the release of the lipokine, 12,13-diHOME.

Elucidating mechanisms to combat obesity and its co-morbidities, including cardiovascular disease (CVD), have become an increasingly important research focus. Brown adipose tissue (BAT) has been identified as an important target to combat obesity, but its role to combat CVD had not been thoroughly investigated. Interestingly, studies have indicated that BAT activity (measured as UCP1 expression) is increased in CVD in mouse models[19-21], but it is not clear if this is detrimental or protective for cardiac function. In this study, we propose that it is the endocrine function of BAT, independent of any measurement of activity, that has a protective effect on cardiac function.

We have now identified a role for the batokine, 12,13-diHOME, to mediate cardiac function both *in vivo* and *in vitro*. Similar to its acute effect on BAT and skeletal muscle, 12,13-diHOME also increases mitochondrial respiration in the isolated cardiomyocyte. Thus, 12,13-diHOME directly increases generation of energy in response to its effect of enhancing the work load of the heart. Our data indicates that 12,13-diHOME mediates beneficial actions on cardiac function via NOS1 within the cardiomyocyte, and these are consistent with previous studies showing that NOS1 enhances cardiac contraction via activation of RyR[46, 47]. Furthermore, sustained treatment with 12,13-diHOME was cardioprotective. In contrast to our data, some studies have indicated a role for 12,13-diHOME to impair cardiac health, however these studies were performed in *ex vivo* or ischemia/reperfusion models, or at concentrations known to be toxic to cardiomyocytes[48-50]. Our data indicate that at supraphysiological concentrations, 12,13-diHOME has a consistent beneficial effect on both *in vivo* and *in vitro* cardiac function and metabolism. Further, our data in human subjects indicate that 12,13-diHOME is decreased in heart disease but positively correlated with ejection fraction, suggesting it as a potential therapeutic. It is important to note that the human functional measurements were only performed in a small population of patients (n=9), only in patients with heart disease, and mostly male patients (n=8 males; n=1 female). Further studies must be performed to fully characterize the correlation of cardiac function and 12,13-diHOME in healthy subjects or other subpopulations. These data suggest that 12,13-diHOME may have beneficial clinical ramifications; however, more long-term studies are be needed to determine the safety and efficacy of 12,13-diHOME treatment.

In conclusion, BAT functions in an endocrine manner to directly modulate the heart via release of the lipokine 12,13-diHOME. The mechanism of action of 12,13-diHOME is similar to exercise (i.e., NOS1) to produce physiological remodeling, as in the “athlete’s” heart. This study uncovers a novel mechanism for metabolic induction of physiological remodeling that underlies the endocrine effects of BAT on cardiac function and provides a new mechanism for 12,13-diHOME as a potential therapeutic modulator for cardiovascular disease.

Supplementary Material

Refer to Web version on PubMed Central for supplementary material.

Acknowledgements:

The authors thanks Drs. Erinn Hade and Beth Lee for statistical discussions. Author contributions are as follows: K.M.P. carried *in vivo* experiments in mice, isolated cardiomyocyte function tests, metabolic testing, measurements of gene expression, and helped write the paper. V.K.S. performed *in vivo* cardiac measurements and helped write the paper. K.R.W. performed experiments in isolated cardiomyocytes. E.A. performed *in vivo* cardiac measurements and performed exercise-training experiments. L.A.B. performed experiments in isolated cardiomyocytes and supervised metabolic experiments in mice. P.V.S. and R.S.D performed metabolic experiments on TNT mice. D.D. and S.D.S. performed TNT experiments. D.H.S. analyzed lipidomics data in mice and humans. P.J.A. and A.C.L. performed exercise-training experiments in mice. V.B. performed lipidomics experiments. M.A.K. and N.R.N. supervised and analyzed lipidomics data. F.Y. assisted with biostatistical analyses. L.M.S., B.H.G, S.R.S., R.E.P., E.D.L., S.V.R., and P.M.C formulated protocols and performed experiments in human subjects. Correspondence for human study should be directed to paul.coen@adventhealth.com. L.E.W. supervised experiments in cardiomyocytes. D.G.P. developed and supervised TNT experiments. M.T.Z. and K.I.S. directed the research project, designed experiments, analyzed data and wrote the paper.

Funding Sources: This work was supported by National Institutes of Health Grants R01-HL138738 to K.I.S., R01-AG060542 to K.I.S., M.T.Z., and P.C.M., DP1DK126199 to D.G.P., and DP2EB028110 to D.G.P., and American Heart Association Grant 17CSA33610078 to K.I.S., M.T.Z., and S.V.R. K.M.P. was supported by T32-HL134616. V.K.S. was supported by American Heart Association 17POST33670923.

Non-standard Abbreviations and Acronyms

BAT	brown adipose tissue
CVD	cardiovascular disease
BMI	body mass index
12,13-diHOME	12,13-dihydroxy-9Z-octadecenoic acid
9,10-diHOME	9,10-dihydroxy-9Z-octadecenoic acid
9-HODE	9-Hydroxyoctadecadienoic acid
TNT	tissue nanotransfection
AUDA	12-(3-adamantan-1-yl-ureido)-dodecanoic acid
t-AUCB	4-[[trans-4-[[(tricyclo[3.3.1.1^{3,7}]dec-1-ylamino)carbonyl]amino]cyclohexyl]oxy]-benzoic acid
UCP1	uncoupling protein 1

sEH	soluble epoxide hydrolase
EPHX	epoxide hydrolase
NOS1	nitric oxide synthase type 1
RyR	ryanodine receptor
OCR	oxygen consumption rates

References

1. Benjamin EJ, Muntner P, Alonso A, Bittencourt MS, Callaway CW, Carson AP, Chamberlain AM, Chang AR, Cheng S, Das SR, et al. Heart Disease and Stroke Statistics-2019 Update: A Report From the American Heart Association. Circulation. 2019;139:e56–e528. [PubMed: 30700139]
2. Colberg SR, Albright AL, Blissmer BJ, Braun B, Chasan-Taber L, Fernhall B, Regensteiner JG, Rubin RR and Sigal RJ. Exercise and type 2 diabetes: American College of Sports Medicine and the American Diabetes Association: joint position statement. Exercise and type 2 diabetes. Medicine Sci Sports Exerc. 2010;42:2282–2303.
3. Ashor AW, Lara J, Siervo M, Celis-Morales C, Oggioni C, Jakovljevic DG and Mathers JC. Exercise Modalities and Endothelial Function: A Systematic Review and Dose-Response Meta-Analysis of Randomized Controlled Trials. Sports Med. 2015;45:279–296. [PubMed: 25281334]
4. Hambrecht R, Wolf A, Gielen S, Linke A, Hofer J, Erbs S, Schoene N and Schuler G. Effect of exercise on coronary endothelial function in patients with coronary artery disease. New Engl J Med. 2000;342:454–460. [PubMed: 10675425]
5. Laughlin MH, Bowles DK and Duncker DJ. The coronary circulation in exercise training. Am J Physiol-Heart C. 2012;302:H10–H23.
6. Pettman TL, Buckley JD, Misan GM, Coates AM and Howe PR. Health benefits of a 4-month group-based diet and lifestyle modification program for individuals with metabolic syndrome. Obes Res Clin Pract. 2009;3:221–235. [PubMed: 24973150]
7. Platt C, Houstis N and Rosenzweig A. Using exercise to measure and modify cardiac function. Cell Metab. 2015;21:227–236. [PubMed: 25651177]
8. Vega RB, Konhilas JP, Kelly DP and Leinwand LA. Molecular Mechanisms Underlying Cardiac Adaptation to Exercise. Cell Metab. 2017;25:1012–1026. [PubMed: 28467921]
9. Lee BA and Oh DJ. The effects of long-term aerobic exercise on cardiac structure, stroke volume of the left ventricle, and cardiac output. J Exerc Rehabil. 2016;12:37–41. [PubMed: 26933658]
10. Roof SR, Tang L, Ostler JE, Periasamy M, Gyorke S, Billman GE and Ziolo MT. Neuronal nitric oxide synthase is indispensable for the cardiac adaptive effects of exercise. Basic Res Cardiol. 2013;108:332–341. [PubMed: 23377961]
11. Stanford KI, Middelbeek RJ, Townsend KL, An D, Nygaard EB, Hitchcox KM, Markan KR, Nakano K, Hirshman MF, Tseng YH et al. Brown adipose tissue regulates glucose homeostasis and insulin sensitivity. J Clin Invest. 2013;123:215–223. [PubMed: 23221344]
12. White JD, Dewal RS and Stanford KI. The beneficial effects of brown adipose tissue transplantation. Mol Aspects Med. 2019; 68:74–81. [PubMed: 31228478]
13. Lynes MD, Leiria LO, Lundh M, Bartelt A, Shamsi F, Huang TL, Takahashi H, Hirshman MF, Schlein C, Lee A, et al. The cold-induced lipokine 12,13-diHOME promotes fatty acid transport into brown adipose tissue. Nat Med. 2017;23:631–637. [PubMed: 28346411]
14. Stanford KI, Lynes MD, Takahashi H, Baer LA, Arts PJ, May FJ, Lehnig AC, Middelbeek RJW, Richard JJ, So K, et al. Cell Metab. 2018;27:1111–1120.e3. [PubMed: 29719226]
15. Dewal RS and Stanford KI. Effects of exercise on brown and beige adipocytes. Biochim Biophys Acta Mol Cell Biol Lipids. 2018;1864:71–78. [PubMed: 29684558]
16. Lehnig AC, Dewal RS, Baer LA, Kitching KM, Munoz VR, Arts PJ, Sindeldecker DA, May FJ, Lauritzen H, Goodyear LJ, et al. Exercise Training Induces Depot-Specific Adaptations to White and Brown Adipose Tissue. iScience. 2019;11:425–439. [PubMed: 30661000]

17. Townsend K and Tseng YH. Brown adipose tissue: Recent insights into development, metabolic function and therapeutic potential. Adipocyte. 2012;1:13–24. [PubMed: 23700507]

18. Villarroya F, Cereijo R, Villarroya J and Giralt M. Brown adipose tissue as a secretory organ. Nat Rev Endocrinol. 2017;13:26–35. [PubMed: 27616452]

19. Thoonen R, Ernande L, Cheng J, Nagasaka Y, Yao V, Miranda-Bezerra A, Chen C, Chao W, Panagia M, Sosnovik DE, et al. Functional brown adipose tissue limits cardiomyocyte injury and adverse remodeling in catecholamine-induced cardiomyopathy. J Mol Cell Cardiol. 2015;84:202–211. [PubMed: 25968336]

20. Panagia M, Chen HH, Croteau D, Iris Chen YC, Ran C, Luptak I, Josephson L, Colucci WS and Sosnovik DE. Multiplexed Optical Imaging of Energy Substrates Reveals That Left Ventricular Hypertrophy Is Associated With Brown Adipose Tissue Activation. Circ Cardiovasc imaging. 2018;11:e007007–007027. [PubMed: 29555834]

21. Raiko J, Orava J, Savisto N and Virtanen KA. High Brown Fat Activity Correlates With Cardiovascular Risk Factor Levels Cross-Sectionally and Subclinical Atherosclerosis at 5-Year Follow-Up. Arterioscler Thromb Vasc Bio. 2020;40:1289–1295. [PubMed: 31941384]

22. Tran TT, Yamamoto Y, Gesta S and Kahn CR. Beneficial effects of subcutaneous fat transplantation on metabolism. Cell Metab. 2008;7:410–420. [PubMed: 18460332]

23. Gallego-Perez D, Pal D, Ghatak S, Malkoc V, Higuita-Castro N, Gnyawali S, Chang L, Liao W-C, Shi J and Sinha M. Topical tissue nano-transfection mediates non-viral stroma reprogramming and rescue. Nat Nanotech. 2017;12:974–988.

24. Zhang F, Hao G, Shao M, Nham K, An Y, Wang Q, Zhu Y, Kusminski CM, Hassan G, Gupta RK, et al. An Adipose Tissue Atlas: An Image-Guided Identification of Human-like BAT and Beige Depots in Rodents. Cell Metab. 2018;27:252–262.e3. [PubMed: 29320705]

25. Wold LE, Relling DP, Colligan PB, Scott GI, Hintz KK, Ren BH, Epstein PN and Ren J. Characterization of contractile function in diabetic hypertensive cardiomyopathy in adult rat ventricular myocytes. J Mol Cell Cardiol. 2001;33:1719–1726. [PubMed: 11549350]

26. Norby FL, Wold LE, Duan J, Hintz KK and Ren J. IGF-I attenuates diabetes-induced cardiac contractile dysfunction in ventricular myocytes. Am J Physiol Endocrinol Metab. 2002;283:E658–666. [PubMed: 12217882]

27. Ziolo MT, Harshbarger CH, Roycroft KE, Smith JM, Romano FD, Sondgeroth KL and Wahler GM. Myocytes isolated from rejecting transplanted rat hearts exhibit a nitric oxide-mediated reduction in the calcium current. J Mol Cell Cardiol. 2001;33:1691–1699. [PubMed: 11549347]

28. Ziolo MT, Dollinger SJ and Wahler GM. Myocytes isolated from rejecting transplanted rat hearts exhibit reduced basal shortening which is reversible by aminoguanidine. J Mol Cell Cardiol. 1998;30:1009–1017. [PubMed: 9618241]

29. Velten M, Gorr MW, Youtz DJ, Velten C, Rogers LK and Wold LE. Adverse perinatal environment contributes to altered cardiac development and function. Am J Physiol Heart Circ Physiol. 2014;306:H1334–340. [PubMed: 24610916]

30. Gorr MW, Velten M, Nelin TD, Youtz DJ, Sun Q and Wold LE. Early life exposure to air pollution induces adult cardiac dysfunction. Am J Physiol Heart Circ Physiol. 2014;307:H1353–360. [PubMed: 25172901]

31. Wu M, Neilson A, Swift AL, Moran R, Tamagnine J, Parslow D, Armistead S, Lemire K, Orrell J, Teich J, et al. Multiparameter metabolic analysis reveals a close link between attenuated mitochondrial bioenergetic function and enhanced glycolysis dependency in human tumor cells. Am J Physiol Cell Physiol. 2007;292:C125–136. [PubMed: 16971499]

32. Zhang B, Davis JP and Ziolo MT. Cardiac Catheterization in Mice to Measure the Pressure Volume Relationship: Investigating the Bowditch Effect. J Vis Exp. 2015:e52618–52625. [PubMed: 26131569]

33. Shettigar V, Zhang B, Little SC, Salhi HE, Hansen BJ, Li N, Zhang J, Roof SR, Ho HT, Brunello L, et al. Rationally engineered Troponin C modulates in vivo cardiac function and performance in health and disease. Nat Commun. 2016;7:10794–10806. [PubMed: 26908229]

34. Che L and Li D. The Effects of Exercise on Cardiovascular Biomarkers: New Insights, Recent Data, and Applications. Adv Exp Med Biol. 2017;999:43–53. [PubMed: 29022256]

35. Ellison GM, Waring CD, Vicinanza C and Torella D. Physiological cardiac remodelling in response to endurance exercise training: cellular and molecular mechanisms. Heart. 2012;98:5–10. [PubMed: 21880653]
36. Pinckard K, Baskin KK and Stanford KI. Effects of Exercise to Improve Cardiovascular Health. Front Cardiovasc Med. 2019;6:69–80. [PubMed: 31214598]
37. Roof SR, Ho HT, Little SC, Ostler JE, Brundage EA, Periasamy M, Villamena FA, Gyorke S, Biesiadecki BJ, Heymes C, et al. Obligatory role of neuronal nitric oxide synthase in the heart's antioxidant adaptation with exercise. J Mol Cell Cardiol. 2015;81:54–61. [PubMed: 25595735]
38. Checa A, Holm T, Sjödin MO, Reinke SN, Alm J, Scheynius A and Wheelock CE. Lipid mediator profile in vernix caseosa reflects skin barrier development. Sci Rep. 2015;5:15740–15747. [PubMed: 26521946]
39. Ohno Y, Nakamichi S, Ohkuni A, Kamiyama N, Naoe A, Tsujimura H, Yokose U, Sugiura K, Ishikawa J, Akiyama M. et al. Essential role of the cytochrome P450 CYP4F22 in the production of acylceramide, the key lipid for skin permeability barrier formation. Proc Natl Acad Sci U S A. 2015;112:7707–7712. [PubMed: 26056268]
40. Ahmad N and Mukhtar H. Cytochrome p450: a target for drug development for skin diseases. J Invest Dermatol. 2004;123:417–425. [PubMed: 15304077]
41. Dong F, Li Q, Sreejayan N, Nunn JM and Ren J. Metallothionein prevents high-fat diet induced cardiac contractile dysfunction: role of peroxisome proliferator activated receptor gamma coactivator 1alpha and mitochondrial biogenesis. Diabetes. 2007;56:2201–2212. [PubMed: 17575086]
42. Endoh M Force-frequency relationship in intact mammalian ventricular myocardium: physiological and pathophysiological relevance. Eur J Pharacol. 2004;500:73–86.
43. Henkin AH, Cohen AS, Dubikovskaya EA, Park HM, Nikitin GF, Auzias MG, Kazantzis M, Bertozzi CR and Stahl A. Real-time noninvasive imaging of fatty acid uptake in vivo. ACS chemical biology. 2012;7:1884–1891. [PubMed: 22928772]
44. Liao J, Sportsman R, Harris J and Stahl A. Real-time quantification of fatty acid uptake using a novel fluorescence assay. J Lipid Res. 2005;46:597–602. [PubMed: 15547301]
45. Covian R, French S, Kusnetz H and Balaban RS. Stimulation of oxidative phosphorylation by calcium in cardiac mitochondria is not influenced by cAMP and PKA activity. Biochim Biophys Acta. 2014;1837:1913–1921. [PubMed: 25178840]
46. Wang H, Viatchenko-Karpinski S, Sun J, Gyorke I, Benkusky NA, Kohr MJ, Valdivia HH, Murphy E, Gyorke S and Ziolo MT. Regulation of myocyte contraction via neuronal nitric oxide synthase: role of ryanodine receptor S-nitrosylation. J Physiol. 2010;588:2905–2917. [PubMed: 20530114]
47. Gonzalez DR, Beigi F, Treuer AV and Hare JM. Deficient ryanodine receptor S-nitrosylation increases sarcoplasmic reticulum calcium leak and arrhythmogenesis in cardiomyocytes. Proc Natl Acad Sci U S A. 2007;104:20612–20617. [PubMed: 18077344]
48. Chaudhary KR, Zordoky BN, Edin ML, Alsaleh N, El-Kadi AO, Zeldin DC and Seubert JM. Differential effects of soluble epoxide hydrolase inhibition and CYP2J2 overexpression on postischemic cardiac function in aged mice. Prostaglandins Other Lipid Mediat. 2013;104–105:8–17.
49. Bannehr M, Lohr L, Gelep J, Haverkamp W, Schunck WH, Gollasch M and Wutzler A. Linoleic Acid Metabolite DiHOME Decreases Post-ischemic Cardiac Recovery in Murine Hearts. Cardiovasc Toxicol. 2019;19:365–371. [PubMed: 30725262]
50. Samokhvalov V, Jamieson KL, Darwesh AM, Keshavarz-Bahaghighat H, Lee TYT, Edin M, Lih F, Zeldin DC and Seubert JM. Deficiency of Soluble Epoxide Hydrolase Protects Cardiac Function Impaired by LPS-Induced Acute Inflammation. Front Pharmacol. 2018;9:1572–1587. [PubMed: 30692927]
51. Albarado DC, McClaine J, Stephens JM, Mynatt RL, Ye J, Bannon AW, Richards WG and Butler AA. Impaired coordination of nutrient intake and substrate oxidation in melanocortin-4 receptor knockout mice. Endocrinology. 2004;145:243–252. [PubMed: 14551222]
52. Stanford KI, Lee MY, Getchell KM, So K, Hirshman MF and Goodyear LJ. Exercise before and during pregnancy prevents the deleterious effects of maternal high-fat feeding on metabolic health of male offspring. Diabetes. 2015;64:427–433. [PubMed: 25204976]

What is new?

- We have identified, for the first time, a role for brown adipose tissue (BAT) to mediate cardiac function via the release of the lipokine 12,13-diHOME
- Increasing 12,13-diHOME increases cardiac function and cardiomyocyte respiration via NOS1.
- This is the first study to determine that 12,13-diHOME levels are decreased in patients with heart disease.

What are the clinical implications?

- This study uncovers a novel mechanism for metabolic induction of physiological remodeling that underlies the endocrine effects of BAT on cardiac function.
- We propose that 12,13-diHOME is a novel potential therapeutic for cardiovascular disease.

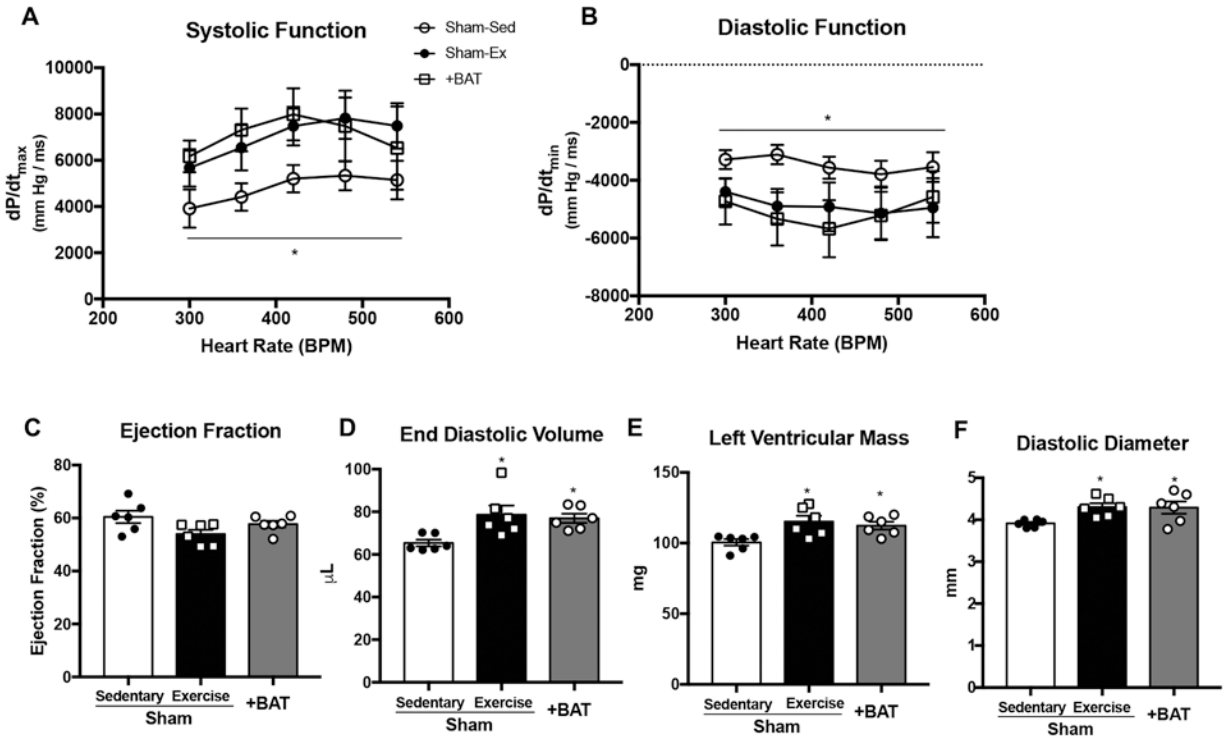

Figure 1. Exercise or increasing BAT mass by transplantation improves cardiac function and structure in mice.

(A) Systolic function and (B) diastolic function measured by *in vivo* cardiac hemodynamics (n=4-6/group). Cardiac function and structure measured by (C) ejection fraction, (D) end diastolic volume, (E) left ventricular mass, and (F) diastolic diameter. Data are mean ± S.E.M (n=6/group). Asterisks represent difference vs. Sham-Sedentary (*P<0.05). Repeated measures two-way ANOVA was used for **A** and **B** with Tukey's multiple comparisons tests; one-way ANOVA was used for **C, D, E, and F** with Tukey's multiple comparisons tests.

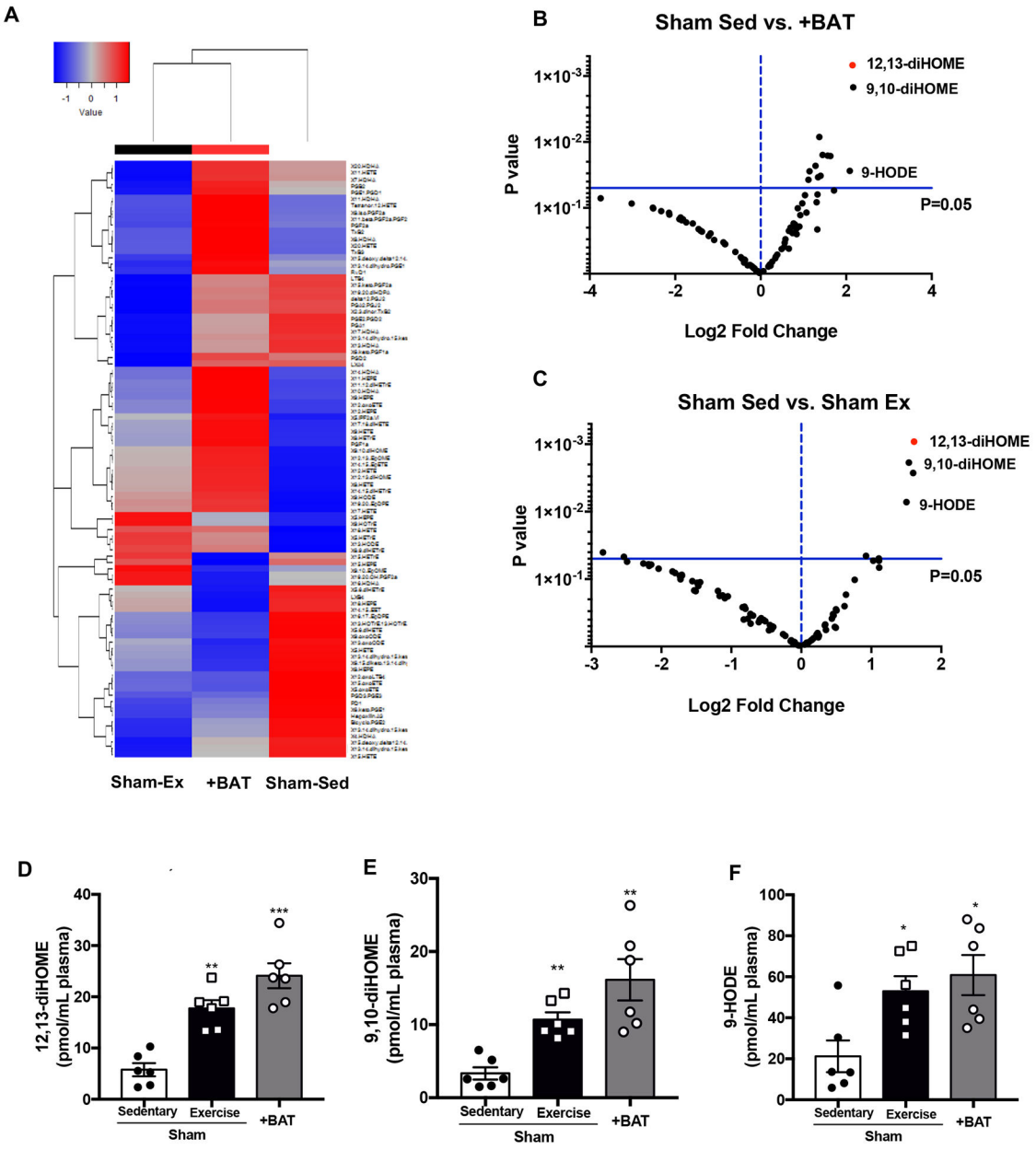

Figure 2. Exercise or transplantation of BAT increases circulating 12,13-diHOME, 9,10-diHOME, and 9-HODE.

(A) Heat map and (B,C) volcano plot representing 88 lipids comparing the fold induction of Sham-Sedentary to the p value; 12,13-diHOME is circled in red. Data are mean ± S.E.M (n=6/group). Plasma concentrations of (D) 12,13-diHOME, (E) 9,10-diHOME, and (F) 9-HODE. Data are mean ± S.E.M (n=6/group). Asterisks represent difference vs. Sham-Sedentary (**P*<0.05; ***P*<0.01; ****P*<0.001). One-way ANOVA was used for **C, D,** and **E** with Tukey's multiple comparisons tests.

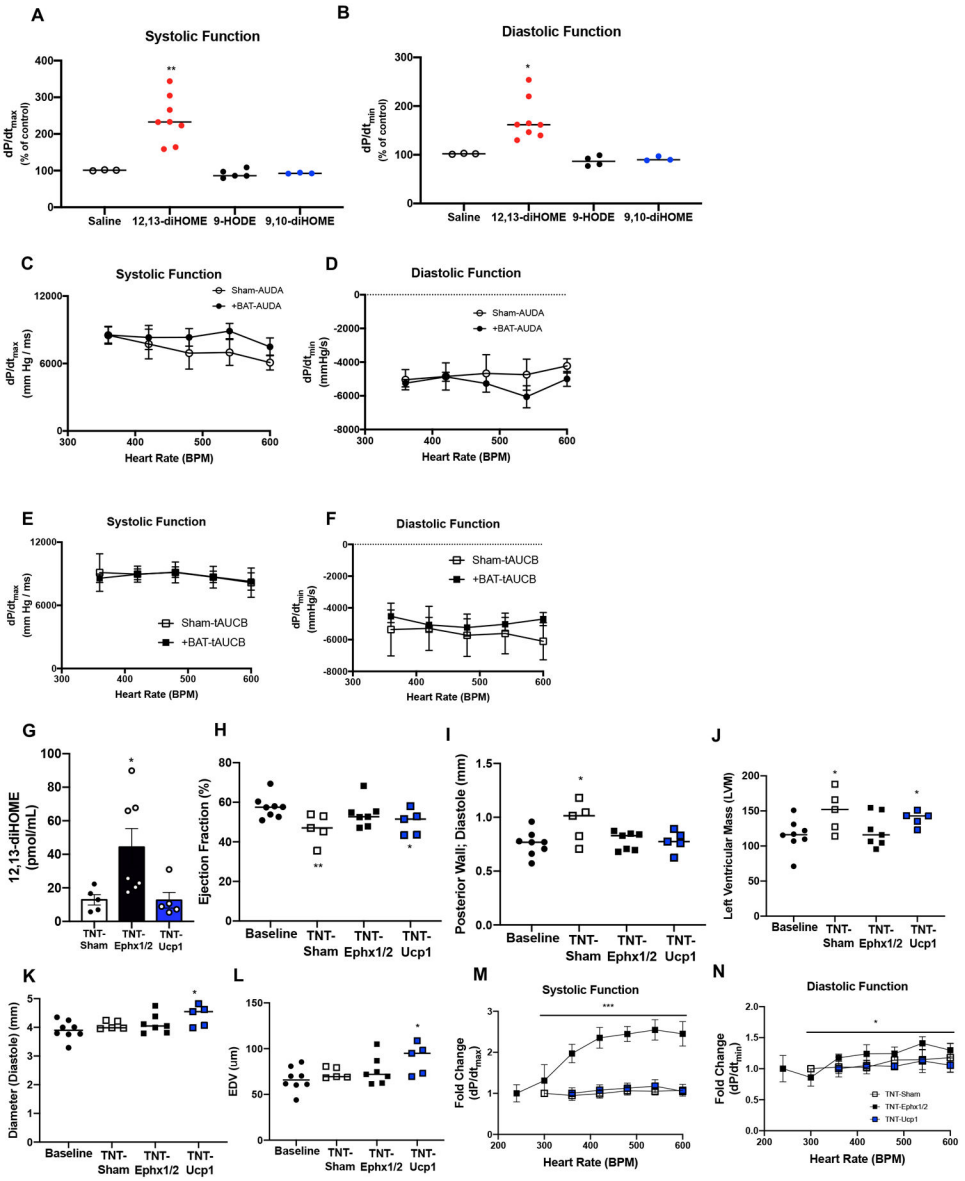

Figure 3. 12,13-diHOME improves *in vivo* cardiac function and structure.

(A) Systolic and (B) diastolic function in mice acutely injected with saline (n=3), 12,13-diHOME (n=8), 9-HODE (n=5), or 9,10-diHOME (n=3). Data are mean ± S.E.M Asterisks represent difference compared to mice injected with saline, 9-HODE, or 9,10-diHOME (**P*<0.05; ***P*<0.01). (C) Systolic and (D) diastolic function measured by *in vivo* cardiac hemodynamics in Sham or +BAT mice fed the sEH inhibitor AUDA. (E) Systolic and (F) diastolic function measured by *in vivo* cardiac hemodynamics in Sham or +BAT mice fed the sEH inhibitor t-AUCB. Data are mean ± S.E.M (n=6/group). (G) 12,13-diHOME in Baseline (n=8), Sham (n=5), TNT-Ephx1/2 (n=7), or TNT-Ucp1 (n=5) mice. Data are mean ± S.E.M Asterisks represent difference compared to Sham (**P*<0.05). Cardiac function and structure measured by (H) ejection fraction, (I) posterior wall thickness, (J) left ventricular mass, (K) diastolic diameter, and (L) end diastolic volume (EDV) was measured in Sham (n=5), TNT-Ephx1/2 (n=7), or TNT-Ucp1 (n=5). Data are mean ± S.E.M Asterisks represent

differences compared to baseline cohort (*P<0.05; **P<0.01). (M) Systolic function and (N) diastolic function measured by *in vivo* cardiac hemodynamics. Data are mean ± S.E.M Asterisks represent difference in TNT-Ephx1/2 compared to all other groups (*P<0.05; **P<0.01; ***P<0.001). Repeated measures two-way ANOVA was used for **C, D, E, F, M,** and **N** with Tukey's multiple comparisons tests. One-way ANOVA was used for **G, H, I, J, K,** and **L** with Tukey's multiple comparisons tests. Kruskal-Wallis test was used for **A** and **B**.

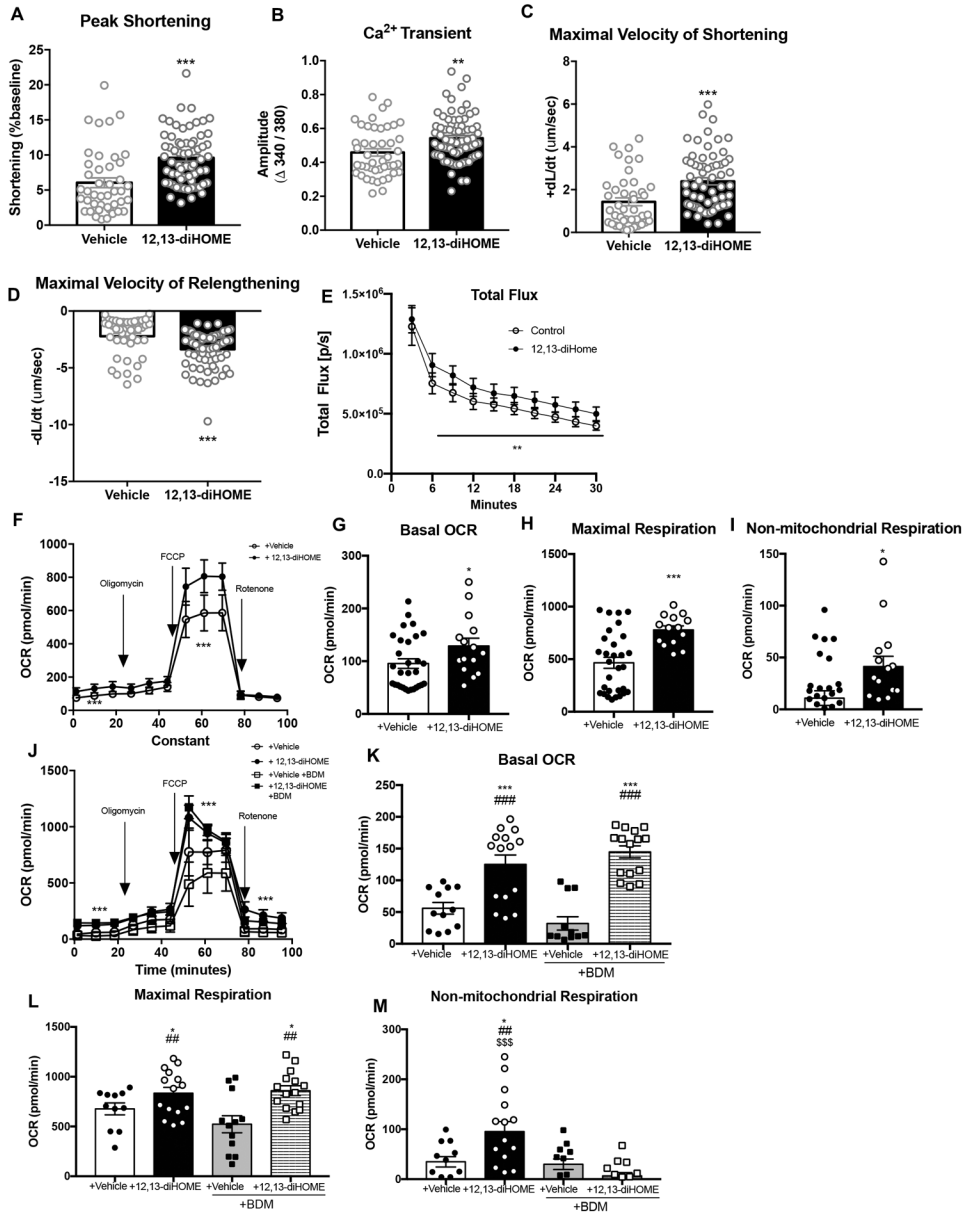

Figure 4. 12,13-diHOME increases function and respiration in isolated cardiomyocytes.

(A) Peak shortening, (B) Ca2+ transient, (C) maximal velocity of shortening, and (D) maximal velocity of relengthening in isolated cardiomyocytes ±12,13-diHOME. Data are mean ± S.E.M (n=4/group; 10-12 myocytes per mouse). Asterisks represent difference compared to vehicle (***P*<0.01; ****P*<0.001). (E) Fatty acid uptake in cardiomyocytes constitutively expressing firefly luciferase that were treated with either 12,13-diHOME or vehicle, as measured by luciferase activity using 10 uM FFA-SS-Luc. Data are mean ± S.E.M (n=9 technical replicate wells per group. Asterisks represent difference compared to vehicle (***P*<0.01). (F) Bioenergetic profile of cardiomyocytes treated with 12,13-diHOME or vehicle. (G) Basal OCR, (H) maximal respiration, and (I) non-mitochondrial respiration were measured. Data are mean ± S.E.M (n=5/group). Asterisks represent differences compared to vehicle (**P*<0.05; ****P*<0.001). (J) Bioenergetic profile of cardiomyocytes

treated with 12,13-diHOME or vehicle with or without BDM. (K) Basal OCR, (L) maximal respiration, and (M) non-mitochondrial respiration were measured. Data are mean ± S.E.M (n=5/group). Asterisks represent differences compared to vehicle (*P<0.05; ***P<0.001), compared to vehicle + BDM (##P<0.01; ###P<0.001), or compared to 12,13-diHOME + BDM ($$$$P$<0.001). Unpaired two-tailed Student's t-test was used for **A**, **B**, **C**, **D, G, H,** and **I.** Two-way ANOVA was used for **E, F** and **J** with Tukey's multiple comparisons tests; one-way ANOVA was used for **K, L,** and **M** with Tukey's multiple comparisons tests.

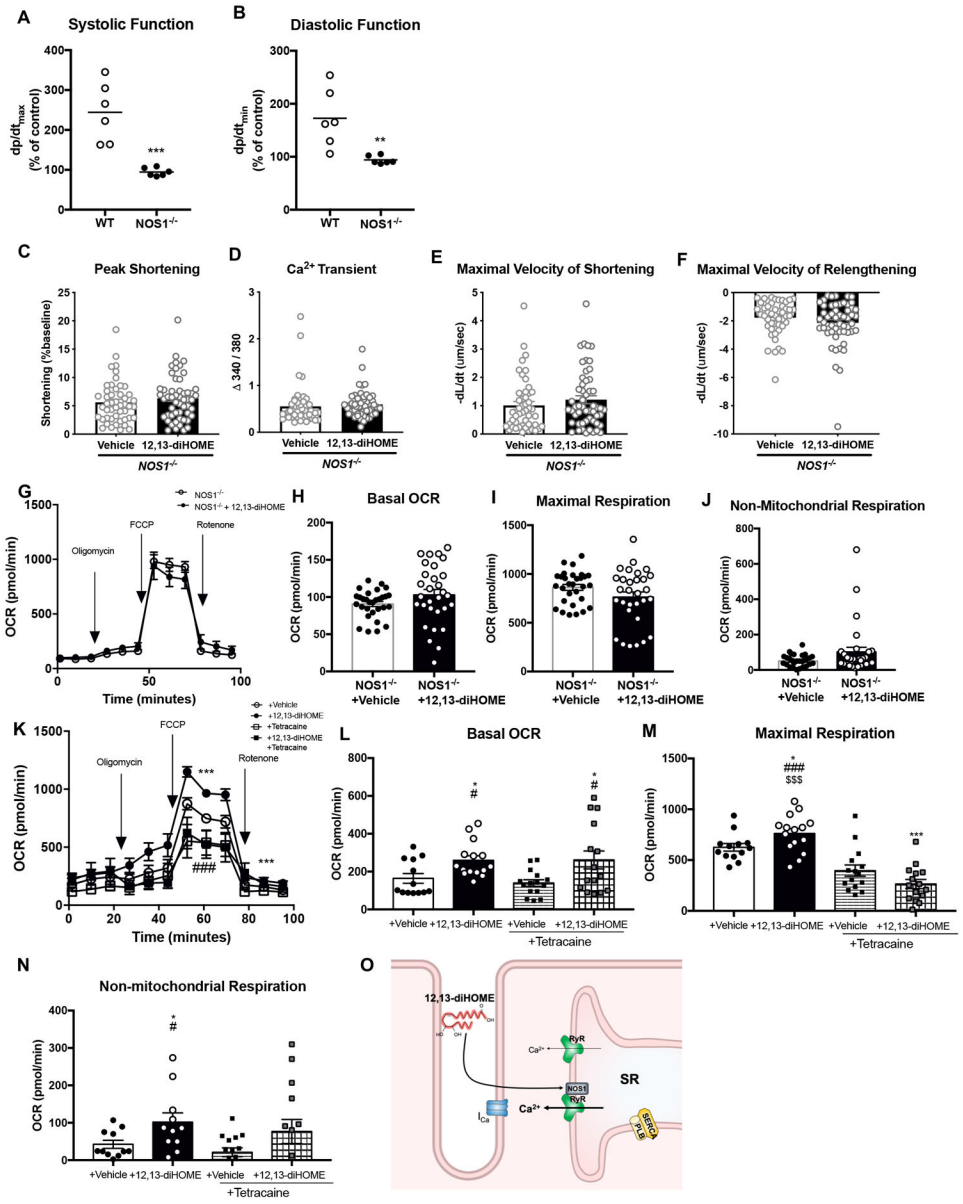

Figure 5. 12,13-diHOME improves cardiac function and respiration via NOS1 and RyR.

(A) Systolic and (B) diastolic function in wild-type (WT) (n=6) or *NOS1*$^{-/-}$ mice (n=6). (C) Peak shortening, (D) Ca2+ transient, (E) maximal velocity of shortening, and (F) maximal velocity of relengthening in isolated cardiomyocytes from *NOS1*$^{-/-}$ mice treated with PBS or 12,13-diHOME. Data are mean ± S.E.M (n=5/group; 5-16 myocytes per mouse). (G) Bioenergetic profile of *NOS1*$^{-/-}$ cardiomyocytes treated with 12,13-diHOME or vehicle. (H) Basal OCR, (I) maximal respiration, and (J) non-mitochondrial respiration were measured. Data are mean ± S.E.M (n=5/group). (K) Bioenergetic profile of cardiomyocytes treated with 12,13-diHOME or vehicle with or without tetracaine. (L) Basal OCR, (M) maximal respiration, and (N) non-mitochondrial respiration were measured. Data are mean ± S.E.M (n=5/group). Asterisks represent differences compared to vehicle (**P*<0.05; ****P*<0.001), compared to vehicle + tetracaine (#*P*<0.05; ###*P*<0.001), or compared to 12,13-diHOME +

tetracaine ($$$*P*<0.001). (O) Proposed model for 12,13-diHOME to regulate cardiac function via NOS1. Unpaired two-tailed Student's t-test was used for **A**, **B**, **C**, **D, E, F, H, I,** and **J.** Two-way ANOVA was used for **G** and **K** with Tukey's multiple comparisons tests. One-way ANOVA was used for **L, M,** and **N** with Tukey's multiple comparisons tests.

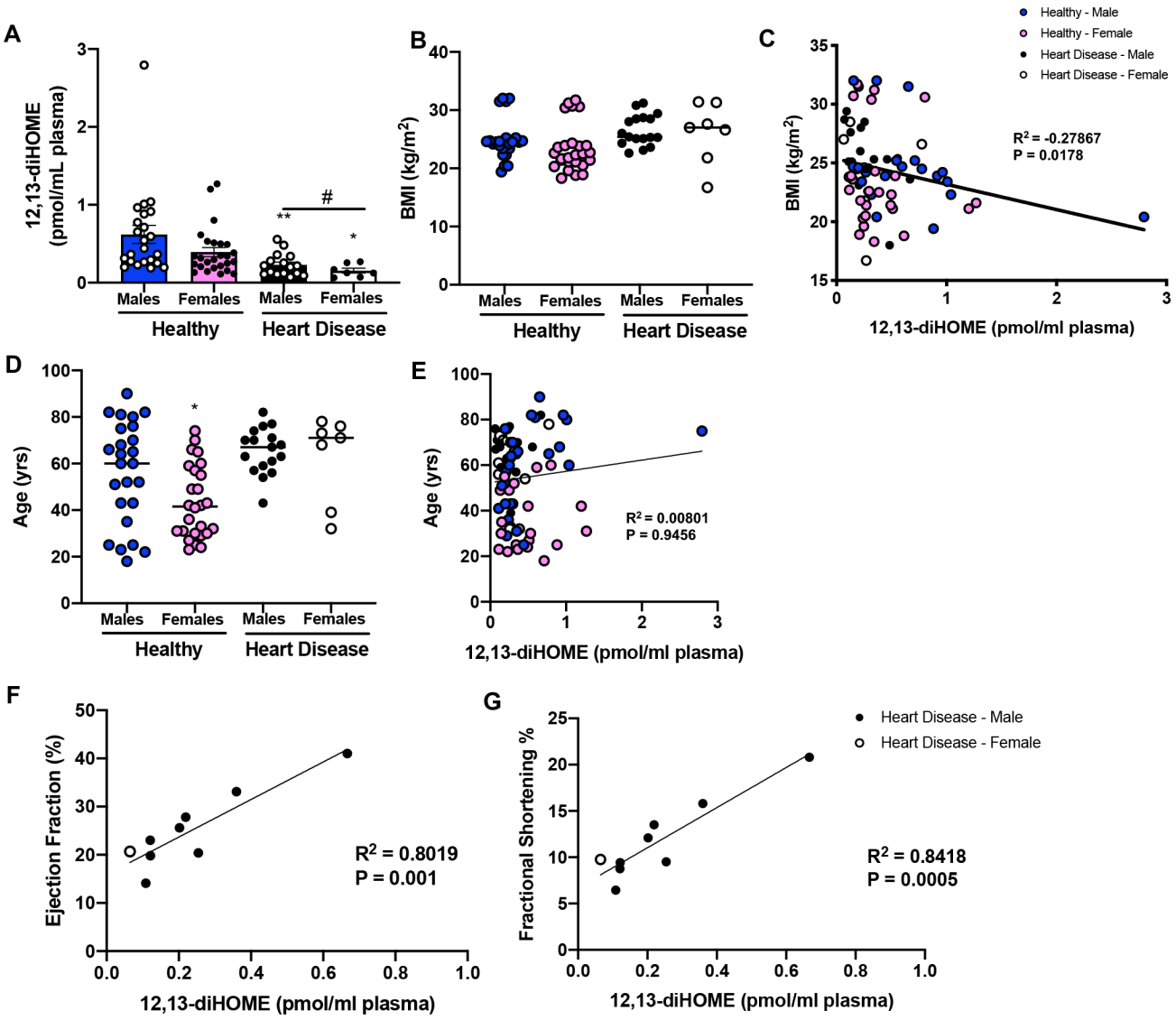

Figure 6. 12,13-diHOME is decreased in human patients with heart disease.

(A) Plasma concentrations of 12,13-diHOME of human subjects (healthy and heart disease). Data are mean ± S.E.M (healthy males n=25; healthy female n=26; males with heart disease n=17; females with heart disease n=7). Asterisks represent differences compared to healthy controls of same gender (**P*<0.05; ***P*<0.01), or an overall effect of heart disease (#*P*<0.05). (B) BMI among groups and (C) correlation among BMI and 12,13-diHOME. (D) Age among groups and (E) correlation among age and 12,13-diHOME. Asterisks represent differences among healthy male and female subjects (**P*<0.05). In a subset of patients with heart disease, (F) ejection fraction and (G) fractional shortening correlated to 12,13-diHOME in plasma. One-way ANOVA was used for **A, B,** and **D** with Tukey's multiple comparisons tests. Spearman's correlation was used for **C** and **E**. Linear regression analyses were used for **F** and **G.**